Quasi-three-dimension Structured Surface-enhanced Raman Scattering Substrates Based on Silver Nanoparticles/ Porous Silicon Hybrid

Thuy Van Nguyen (vannt@ims.vast.ac.vn)
Institute of Materials Science, Vietnam Academy of Science and Technology
Duc Chinh Vu
Institute of Materials Science, Vietnam Academy of Science and Technology
Huy Bui
Institute of Materials Science, Vietnam Academy of Science and Technology
Thanh Binh Pham
Institute of Materials Science, Vietnam Academy of Science and Technology
Thi Hong Cam Hoang
University of Science and Technology of Hanoi, Vietnam Academy of Science and Technology
Van Hai Pham
Hanoi National University of Education
Van Hoi Pham
Institute of Materials Science, Vietnam Academy of Science and Technology

Research Article

Keywords: Surface-enhanced Raman scattering (SERS), silver nanoparticles/porous silicon hybrid structures, Diphenylamine (DPA)

Posted Date: September 29th, 2021

DOI: https://doi.org/10.21203/rs.3.rs-936218/v1

Abstract

Surface-enhanced Raman scattering (SERS) is a powerful spectroscopic technique for ultrasensitive and selective bio-chemical detection due to its capability of providing “fingerprint” information of molecular structures in low concentrations even at single molecular level. In this work, we present the silver nanoparticles/porous silicon (AgNPs/PSi) hybrid structures as SERS substrates prepared by a fast, straightforward and effective method using the PSi immersion plating in silver nitrate ($AgNO_3$) solution. The nano-silvers can simultaneously grow on the surface and nano-pillars of porous silicon making quasi-three-dimension (quasi-3D) structural SERS substrate that has a large surface area to adsorb moleculars for SERS measurement. The proposed SERS substrate can detect Diphenylamine (DPA) with ultralow concentration of 10^{-9} M (~0.17 ppb), which would have higher enhancement than 2D surface SERS based on nano-silver deposited on silicon substrate and other electrochemical sensors.

1. Introduction

Surface-enhanced Raman scattering (SERS), as a powerful chemical and biological analytical technique, has gained more interest from researchers because of its high sensitivity and molecular specificity[1,2]. Many researchers have successfully used Raman spectrometry method to detect pesticide residues based on SERS using noble nano-metals, especially gold nano-structures for controlling pollution of fruits and food[3,4]. Since being accidentally discovered in 1956 by Arthur Uhlir and Ingeborg Uhlir, porous silicon (PSi) has been widely used for sensors, such as biological sensors[5,6], electrochemical sensors[7], and optical sensors[8]. PSi exhibits key features for label-free sensor and biochemical sensor applications due its easy, fast, and low-cost fabrication, tunable shape, pore size, porosity and thickness[9], high surface area of approximately 170 $m^2.cm^{-3}$ [10], detection of molecules/target analytes via the photoluminescent spectrum or as a wavelength shift in the reflectivity spectrum, biocompatibility with existing silicon based microelectronic technology for biological applications. Moreover, PSi was miniaturized and integrated in micro-electromechanical systems (MEMS) using silicon-based technology and portable devices[11]. In recent years, PSi hybrid sensors using quantum dots (QDs), metal nanoparticles (MNPs) or both QDs/MNPs have drawn much attention for sensitivity enhancement and detection of ultra-low concentration of molecules. On the whole, PSi MNPs hybrids were utilized for SERS applications. SERS is a powerful detection technique which is capable of detecting and identifying a small number of molecules[12,13], environmental monitoring, biochemical analysis, food safety and many other fields[14,15,16]. The effect of SERS enhancement depends on two important parameters, namely noble metals and the surface microstructures of the active substrates[17]. Among the various noble metals, silver nanoparticles (AgNPs) have attracted the interest of many researchers due to their broadband plasmonic resonance in visible and near-IR spectral ranges, high electrical and thermal conductivity, high local surface plasmonic resonance (LSPR) performance, chemical stability and easy preparation[18,19,20]. PSi is employed as a template for AgNPs deposition because the Si-H terminated group and its location on the surface of PSi or the roughness surface are capable of reducing silver ions from its salt solutions without adding any

reducing agent[21]. AgNPs/PSi hybrids have been applied as a sensing substrate for SERS with Raman enhancement of more than ten orders of magnitude[22].

Diphenylamine (DPA) is a choice for testing activity of proposed SERS substrate because it is an organic compound with high antioxidant properties widely employed in rubber and elastomer industry, dye mordant and reagent and a pre- or post-harvest scald inhibitor for some fruits[23,24], which can seriously pollute the living environment. Because of its low solubility in water, it is not completely removed from the agricultural crops and therefore, residues of DPA have been detected in milk of animals (cow, sheep, goat, and water buffalo), fruits (pears and apples) and waste water from industrial processes[25,26]. The presence of DPA residues in foods and environment can be considered as a hazard to human health since it is classified as a probable human carcinogen[27]. According to literature in foodstuffs, the maximum allowed concentration for DPA is between 5 and 10 mg.kg-1 (5–10 ppm) for apples and pears[28], so that the analytical techniques for accurate detection of DPA in fruit, food, and environmental water samples are important and necessary for living safety. Several methods have been reported to be used such as high performance liquid chromatography (HPLC)[29,30], gas chromatography (GC)[31] and spectrophotometry[32]. Although spectrophotometric methods are more useful for determination of DPA at low concentration level, these methods require treatment of the samples, time consuming and expensive instruments. Thus, there has been an urgent requirement for a simple, low cost, highly selective and sensitive, and highly accurate quantitative analysis method for the detection of DPA in practice.

In this paper, we present an effective method, i.e. the immersion plating method to prepare AgNPs/PSi hybrid as a sensing substrate for SERS with quasi-three-dimension structure. The materialization of AgNPs/PSi was confirmed by the field emission scanning electron microscope (FE-SEM), Energy dispersive X-Ray spectroscopy (EDX) and High Resolution X-Ray Diffractometer. The SERS activity of AgNPs/PSi substrates was applied to detect the residue of DPA with limit of detection (LOD) of 10^{-9} M (~ 0.17 ppb). The very low LOD of SERS based on AgPNs/PSi structures may be due to the huge number of molecules adsorbed into the large active area of the quasi-three-dimension structures. The proposed SERS sensors demonstrate a big potential to control the environmental and food pollution from DPA according EU regulations.

2. Experiment

2.1 Materials

Monocrystalline silicon wafers used in this investigation were p-type, Boron doped, with a typical resistivity 0.002-0.004 Ω.cm, (100) orientations and 500-550 µm thickness, obtained from CrysTec GmbH, Germany. The electrolyte solution contains 48 wt% Hydrofluoric acid (HF, Merck Milllipore) and 99.9% Ethanol absolute (Merck Milllipore) in a volume ratio of 1:2. Silver nitrate ($AgNO_3$, ≥99.0%) was dissolved in ethanol at concentration of 10^{-2} M, purchased from Sigma-Aldrich. Diphenylamine (DPA, 99.99%) was purchased from Sigma-Aldrich and dissolved in ethanol to obtain the standard stock with concentration

of 10^{-1} M. Then, the standard analyte solution was dissolved in ethanol to prepare analyte solutions of a wide range of concentrations 10^{-3} to 10^{-9} M. Analyte solutions with volumes of 10 µL were dropped onto the AgNPs/PSi surface and dried in the air to form the samples for the Raman spectroscopic measurements.

2.2 Formation of the porous silicon

The porous silicon structures with round area of 1.0 cm diameter were fabricated by the anodic electrochemical method, as reported in our previous work[8]. The etching process was carried out using Teflon cell and a programmable DC power supply (Agilent E3640A); platinum mesh was used as the cathode electrode and silicon wafer acts as the anode, as illustrated in Figure 1. All of the PSi substrates in this work were prepared at a current density of 50 mA/cm^2 for a duration of 2 min with the etching electrolyte solution composed of a mixture of HF/ethanol = 1:2.

2.3 Formation of AgNPs on porous silicon structures and on silicon surface

The synthesis and deposition of nano Ag-particles on the silicon surface and PSi samples were performed by using a simple and quick immersion plating process. The single crystalline silicon wafer was ultrasonically rinsed with isopropanol, methanol and deionized water in sequence. After the ultrasonic treatment, the silicon wafer was dipped into 5% HF aqueous solution for 5 min to form hydrogen-terminated surfaces. Then the silicon wafer was immediately immersed into a solution containing 4.8 M HF and 10^{-2} M $AgNO_3$ for 2 min to form silver nanoparticles. After that, the silicon substrate was rinsed with deionized water to remove the extra silver cations and then dried by a gentle flow of nitrogen gas. The synthesis and deposition of AgNPs on the PSi samples were carried out by following steps: The as-formed PSi samples, that washed with deionized water and dried in air, were dipped into an ethanol solution of $AgNO_3$ with a concentration of 1 mM for different immersion times of 5, 10, 20, and 30 minutes at room temperature to synthesize AgNPs/PSi hybrid structures.

Due to Si-H groups on the silicon and/or PSi surfaces, Ag^+ ions can be easily reduced to AgNPs[33]. The silver reduction process showed according to the following equations[34]:

$$Si + 6HF \rightarrow H_2SiF_6 + 4H^+ + 4e^- \quad (1)$$

$$Ag^+ + e^- \rightarrow Ag \quad (2)$$

Based on these reactions, the silver nuclei eventually deposited on the surface of silicon. Besides, because of the ultrafast silver growth rate, the Ag aggregated on the silicon and/or PSi structures at extremely short dipping time. Afterward, the AgNPs/Si and AgNPs/PSi substrates were washed with deionized water and dried under the stream of nitrogen gas.

2.4 Characterizations and SERS measurement

The reflectance spectra of bare PSi were characterized by a spectrometer (USB-4000, Ocean Optics) and a halogen light source (HL-2000 Ocean Optics). Structural and morphological properties of as-formed PSi and AgNPs/PSi hybrid structure surface were examined by the FE-SEM (FE-SEM, Hitachi S-4800, Japan), and EDX. The crystalline structure of AgNPs/PSi was obtained by High Resolution X-Ray Diffractometer X ARL EQUINOX 5000 Series, power diffraction system with Cu-Kα x-ray tube (λ=1.540560 Å) was used. Raman spectra of detecting DPA were obtained using Raman microscope system (Horiba Scientific LabRAM HR Evolution), equipped with laser of 532 nm-wavelength emission for excitation. For each spectrum, the low laser power of 1.5 mW was used to avoid sample heating effects and the integration time was set at 10 s. The laser spot on the sample surface was about 1 μm in diameter.

3. Results And Discussion

Figure 2a shows the cross-sectional SEM image of PSi layer obtained after the etching process. Thickness of the PSi layer was approximately 4 μm. The top view SEM image presented in figure 2b reveals that the PSi layer is composed of a network of nano-pores with sponge-like structure. It is clear that the pores are uniformly distributed and have nearly circular shapes. The pore size distribution ranges from 5 nm to 45 nm with the peak distribution has the maximum value within the range from 20 nm to 25 nm as shown in figure 2c, and figure 2d depicts the reflectance spectrum of PSi structure with several peaks like Fabry-Perot resonant spectrum in the wavelength range from 500 nm to 1000 nm.

Figure 3 presents the morphology of nano-silver coating layer on the silicon surface after 2 minutes immersed into 4.8 M HF and 10^{-2} M $AgNO_3$ solution. The silver coating layers can be generated from nano-particle, nano flower-like (figure 3a) and nano-dendrite (figure 3b) forms. The average sizes are of 50 nm for nano-particles, of 200 nm for nano flower-like, and the length of nano-dendrites is of 1500 nm.

Figures 4a and 4c illustrate the SEM images of the AgNPs growths on the PSi surface and on the PSi-nanopillars, respectively, in which the samples prepared by immersion plating of the bare PSi into 1 mM $AgNO_3$ solution for 20 min at room temperature.

The AgNP size distribution on the PSi surface is homogeneous with an average size of 25 nm, but the AgNP size on the nanopillars may be smaller. The existences of AgNP deposited on the PSi surface and on the nanopillars measured by the energy dispersive X-ray spectroscopy (EDX) are demonstrated in figures 4b and 4d. The appearance of the Si and O elements is obvious in EDX spectra because of the Si substrate and the oxidation of Si[35,36]. The evidence of nano-silver deposited on the nano-pillars inside the porous silicon structures shows that the hybrid AgNPs/PSi substrates would be to have larger active surface area for SERS measurement as quasi-three-dimension (quasi-3D) structure in comparison with two-dimension (2D) structure of AgNPs/Si. Figure 4e shows the XRD analysis of AgNPs deposited on PSi structure. There are two diffraction peaks at 38.5^o and 44.7^o corresponding to the reflection of 111 and 200 planes of the face-centred cubic (FCC) silver nanoparticles, respectively. These two peaks were labelled according to the standards of diffraction card of the Joint Committee on Power Diffraction Standards (JCPDS) file No. 01-073-6859.

From various parameters influenced on the morphology of AgNPs, the concentration of metallic salt solution and the deposition duration play key roles for deposition of nano-Ag on the PSi surface[23,37]. Figure 5 presents homogenous growth of nano-silver at different immersion times of (5, 10, 30) minutes. Figures 5a and 5b show that only an Ag partial coverage of the porous surface of 70-80% is obtained for immersion times of 5 and 10 minutes. In these cases, the particles are partially conjugated, forming a fractal-like network of large islands of Ag at early stages (5 and 10 minutes). In between, much smaller particles are observed on the underlying PSi substrate. This duration suggests that the nucleation of Ag nanoparticles started almost simultaneously at numerous sites across the whole PSi structure. Nevertheless, the existence of small Ag particles demonstrates that the nucleation and growth process are going on. Using the immersion time of 30 min, the PSi surface is covered of 98% with a dense layer composed of nanometer-size Ag particles as illustrated in figure 5c. The size is related to the number and the gap between the AgNPs, where at the early soaking times the large islands of Ag are formed and the gap between AgNPs is in the range from 50 to 160 nm. After dipping for 30 minutes, many overlapping AgNPs are observed as shown in figure 5c. For investigation on how overlapping AgNPs influenced to SERS effect, we used the samples with immersion time of 20 minutes as shown in figure 4a.

In order to verify the SERS activity of AgNPs deposited on the silicon and PSi substrates in the trace detection of toxic substances, DPA was selected as a model analyte due to its high toxicity and widespread use in agriculture. In addition, the DPA is a highly chemical reactive compound due to the imine hydrogen atom, which can easily be replaced electrophilically[25], a reaction can be used for adsorbing DPA into PSi, where the molecular structures are of SiO_x (x<2) and/or Si-O-H.

Figure 6 shows Raman spectra of DPA molecules absorbed on the AgNPs/PSi substrate excited at the wavelength of 532 nm with a DPA concentration of 10^{-3}M (line a), and of DPA in the solid form (line b). The change of Raman spectrum from SERS measurement in the spectral peaks compared to common Raman measurement can be explained by chemical interaction between nano-silvers and DPA molecules. Some peaks with typical strong intensity at 517 cm^{-1}, 913 cm^{-1}, 1177 cm^{-1} and 1620 cm^{-1} correspond to vibration modes of C=C stretching vibrations, C-H out of plane ring wagging, C-H in plane outer ring angle bending and C-C/C-N in plane stretching[38,39]. Two primary characteristic Raman peaks of DPA at 339 cm^{-1} and 1297 cm^{-1} are assigned to C-N-C in plane angle bending and C-N in plane stretching[38]. The strong other ones at 807 cm^{-1}, 1373 cm^{-1} and 1588 cm^{-1} are attributed to C-H out of plane ring wagging, C-C/C-N in plane stretching and C=C in plane stretching, respectively[40]. The intensity of the peak at 1620 cm^{-1} was chosen as the parameter to characterize the SERS signals.

Figures 7a and 7c present the SERS signals of DPA excited at 532 nm wavelength with varying concentrations from 10^{-9} M to 10^{-3} M adsorbed on the AgNPs/Si and AgNPs/PSi substrates, respectively. It is shown that SERS is attained at all DPA concentrations of the range from 10^{-9} M to 10^{-3} M and the basic SERS signals of DPA molecules can still be identified at the extremely low concentration of 10^{-9} M. A linear dependence between the logarithmic concentration of DPA and the intensity of the peak at

1620 cm^{-1} was observed for SERS substrates based on AgNPs/Si (figure 7b), and on AgNPs/PSi (figure 7d). These results show a good linearity (R^2 = 0.9979) and the limit of detection (LOD) is of 10^{-9} M.

Figure 8a demonstrates the SERS intensities for DPA with a concentration of 10^{-9} M adsorbed on the AgNPs/Si and AgNPs/PSi substrates. The Raman signal obtained from AgNPs/PSi is 5 times higher than that from AgNPs/Si. Figure 8b shows the dependence of Raman intensities upon DPA concentration in the range of 10^{-3}-10^{-9} M. The Raman intensity from the hybrid nano-Ag/PSi structure is several times higher than that from nano-Ag/Si substrate. This phenomenon can be explaind by the large active surface area of the nano-Ag/PSi as a quasi-three-dimension (quasi-3D) structure in comparison with 2D structure from the nano-Ag/Si, because the nano-Ag can be simultaneously deposited on the surface of the PSi substrate and on the nano-pillars of the PSi structures. Further work is needed in order to control the nano-pillar sizes for obtaining the optimum active surface of hybrid nano-Ag/porous silicon structural SERS substrates.

Table 1 shows the limit of detection (LOD) for DPA measuring by different methods. The electrochemical sensors based on different substrates possess the LOD of 10^{-4}–10^{-8} M, and the portable Raman spectrometer without the SERS effect has the LOD of 10^{-3} M. Our result of LOD obtained from SERS substrates based on the hybrid AgNPs/PSi structures is below 10^{-9} M. Thus, the hybrid AgNPs/PSi SERS substrate exhibits an ultrasensitive detection of DPA down to 10^{-9} M, which indicates a good method for toxic molecular sensing.

Table 1. Summary of limit of detection (LOD) for DPA obtained from different technics.

Techniques	Detection Limit (M)	Ref&Year
Thin-film Electrochemical sensor	3.9 x 10^{-6} M	[23] 2014
Portable Raman spectrometer	14.43 x 10^{-3} M	[41] 2019
Molecularly imprinted polymers (MIP) technique based Carbon paste electrochemical sensor	10^{-4} M	[42] 2017
Electrochemical sensor based on reduced Graphene Oxide/Fe3O4-molecularly imprinted Polymer	5x 10^{-8} M	[43] 2018
Surface-enhanced Raman scattering based on AgNPs/PSi	Below 10^{-9} M	This work

4. Conclusion

In summary, the AgNPs/PSi SERS substrates having quasi-three-dimension structure were successfully prepared by an effective immersing method in an $AgNO_3$ solution. The quasi-3D structural SERS substrates based on the hybrid nano-Ag/PSi have been employed to detect the residue of DPA in the

concentration range of 10^{-9} -10^{-3} M and the Raman intensities from the quasi-3D structural SERS substrates are about 5 times higher than that from the nano-Ag/Si 2D-substrates. The limit-of-detection for DPA residues is below 10^{-9} M, to our knowledge, is the lowest concentration detected by PSi-based SERS substrates. The quasi-3D structures based on the hybrid nano-silver on porous silicon, which are high-sensitive SERS substrates, have a huge potential for applications in the SERS field, and can be characterized by easy and low-cost fabrication.

Declarations

Acknowledgements

This research is funded by Vietnam National Foundation for Science and Technology Development (NAFOSTED) under grant number 103.03-2019.310 and Institute of Materials Science (IMS)-Vietnam Academy of Science and Technology (VAST) under grant number CS.06/21-22.

Author contributions

Thuy Van Nguyen, Van Hoi Pham and Huy Bui devised the main ideas of the project. Thuy Van Nguyen, Van Hoi Pham and Thi Hong Cam Hoang wrote the manuscript. Thuy Van Nguyen, Duc Chinh Vu, Huy Bui, Thanh Binh Pham, Van Hai Pham, Thi Hong Cam Hoang and Van Hoi Pham contributed to do experiments and revised the manuscript.

Competing interest statement

The authors declare no competing interests.

References

1. Yu, Y., Xiao, T. H., Wu, Y., Li, W., Zeng, Q. G., Long, L., Li, Z. Y. Roadmap for single-molecule surface-enhanced Raman spectroscopy. *Adv. Photonics* **2**, 014002, DOI: https://doi.org/10.1117/1.AP.2.1.014002 (2020).
2. Almehmadi, L. M., Curley, S. M., Tokranova, N. A., Tenenbaum, S. A., and Lednev, I. K. Surface Enhanced Raman Spectroscopy for Single Molecule Protein Detection. *Sci. Rep.* **9**, 12356, DOI: https://doi.org/10.1038/s41598-019-48650-y (2019).
3. Chen, W., Long, F., Song, G., Chen, J., Peng, S., and Li, P. Rapid and sensitive detection of pesticide residues using dynamic surface-enhanced Raman spectroscopy. *J. Raman Spectrosc.* **51**, 611–618, DOI: https://doi.org/10.1002/jrs.5823 (2020).
4. Liu, B., Zhou, P., Liu, X., Sun, X., Li, H., and Lin, M. Detection of Pesticides in Fruits by Surface-Enhanced Raman Spectroscopy Coupled with Gold Nanostructures. *Food Bioprocess Technol.* **6**, 710–718, DOI: https://doi.org/10.1007/s11947-011-0774-5 (2013).

5. Abu-Thabit, N. and Ratemi, E. Hybrid Porous Silicon Biosensors Using Plasmonic and Fluorescent Nanomaterials: A Mini Review. *Front. Chem.* **8**, 454, DOI: https://doi.org/10.3389/fchem.2020.00454 (2020).
6. Arshavsky-Graham, S., Massad-Ivanir, N., Segal, E., and Weiss, S. Porous Silicon-Based Photonic Biosensors: Current Status and Emerging Applications. *Anal. Chem.* **91**, 441-467, DOI: https://doi.org/10.1021/acs.analchem.8b05028 (2019).
7. Ensafi, A. A., Abarghoui, M. M., and Rezaei, B. A new electrochemical sensor based on porous silicon supported Pt–Pd nanoalloy for simultaneous determination of adenine and guanine. *Sensors Actuators B Chem.* **204**, 528–535, DOI: https://doi.org/10.1016/j.snb.2014.08.009 (2014).
8. Bui, H., Pham, V. H., Pham, V. D., Hoang, T. H. C., Pham, T. B., Do, T. C., Ngo, Q. M. & Nguyen, T. V. Determination of low solvent concentration by nano-porous silicon photonic sensors using volatile organic compound method. *Environ. Technol.* **40**, 3403-3411, DOI: https://doi.org/10.1080/09593330.2018.1474268 (2019).
9. Kumar, P. and Huber, P. Effect of Etching Parameter on Pore Size and Porosity of Electrochemically Formed Nanoporous Silicon. *J. Nanomater.* **2007**, 089718, DOI: https://doi.org/10.1155/2007/89718 (2007).
10. Herino, R. Properties of porous silicon. 1st edn. (INSPEC/IEE, London) (1997).
11. Fischer, A. C., Forsberg, F., Lapisa, M., Bleiker, S. J., Stemme, G., Roxhed, N. & Niklaus, F. Integrating MEMS and Ics. *Microsyst. Nanoeng.* **1**, 15005, DOI: https://doi.org/10.1038/micronano.2015.5 (2015).
12. Luong, T. Q. N., Cao, T. A., and Dao, T. C. Low-concentration organic molecules detection via surface-enhanced Raman spectroscopy effect using Ag nanoparticles-coated silicon nanowire arrays. *Adv. Nat. Sci. Nanosci. Nanotechnol.*, **4**, 015018, https://doi.org/10.1088/2043-6262/4/1/015018 (2013).
13. Bandarenka, H. V., Girel, K. V., Zavatski, S. A., Panarin, A., and Terekhov, S. N. Progress in the Development of SERS-Active Substrates Based on Metal-Coated Porous Silicon. *Materials (Basel).* **11**, 852, DOI: https://doi.org/10.3390/ma11050852 (2018).
14. Qu, L. L., Liu, Y. Y., He, S. H., Chen, J. Q., Liang, Y., and Li, H. T. Highly selective and sensitive surface enhanced Raman scattering nanosensors for detection of hydrogen peroxide in living cells. *Biosens. Bioelectron.* **77**, 292–298, DOI: https://doi.org/10.1016/j.bios.2015.09.039 (2016).
15. Kadian, S., Manik, G., Das, N., Nehra, P., Chauhan, R. P., and Roy, P. Synthesis, characterization and investigation of synergistic antibacterial activity and cell viability of silver–sulfur doped graphene quantum dot (Ag@S-GQDs) nanocomposites. *J. Mater. Chem. B* **8**, 3028–3037, DOI: https://doi.org/10.1039/C9TB02823D (2020).
16. Muhammad, M., Yan, B., Yao, G., Chao, K., Zhu, C., and Huang, Q. Surface-Enhanced Raman Spectroscopy for Trace Detection of Tetracycline and Dicyandiamide in Milk Using Transparent Substrate of Ag Nanoparticle Arrays. *ACS Appl. Nano Mater.* **3**, 7066–7075, DOI: https://doi.org/10.1021/acsanm.0c01389 (2020).

17. Feng, F., Zh,i G., Jia, H. S., Cheng, L., Tian, Y. T., and Li, X. J. SERS detection of low-concentration adenine by a patterned silver structure immersion plated on a silicon nanoporous pillar array. *Nanotechnology* **20**, 295501, DOI: https://doi.org/10.1088/0957-4484/20/29/295501 (2009).
18. Alwan, A. M., Yousif, A. A., and Wali, L. A. A Study on the Morphology of the Silver Nanoparticles Deposited on the n-Type Porous Silicon Prepared Under Different Illumination Types. *Plasmonics* **13**, 1191–1199, DOI: https://doi.org/10.1007/s11468-017-0620-3 (2018).
19. Parnsubsakul, A., Ngoensawat, U., Wutikhun, T., Sukmanee, T., Sapcharoenkun, C., Pienpinijtham, P., Ekgasit, S. Silver nanoparticle/bacterial nanocellulose paper composites for paste-and-read SERS detection of pesticides on fruit surfaces. *Carbohydr. Polym.* **235**, 115956, DOI: https://doi.org/10.1016/j.carbpol.2020.115956 (2020).
20. Nemciauskas, K., Traksele, L., Salaseviciene, A., and Snitka, V. A silicon membrane-silver nanoparticles SERS chip for trace molecules detection. *Microelectron. Eng.* **225**, 111282, DOI: https://doi.org/10.1016/j.mee.2020.111282 (2020).
21. Harraz, F. A., Ismail, A. A., Bouzid, H., Al-Sayari, S. A., Al-Hajry, A., and Al-Assiri M. S. Surface-enhanced Raman scattering (SERS)-active substrates from silver plated-porous silicon for detection of crystal violet. *Appl. Surf. Sci.* **331**, 241–247, DOI: https://doi.org/10.1016/j.apsusc.2015.01.042 (2015).
22. Virga, A., Rivolo, P., Frascella, F., Angelini, A., Descrovi, E., Geobaldo, F., Giorgis, F. Silver Nanoparticles on Porous Silicon: Approaching Single Molecule Detection in Resonant SERS Regime. *J. Phys. Chem. C* **117**, 20139–20145, DOI: https://doi.org/10.1021/jp405117p (2013).
23. Granado, V. L. V., Gutiérrez-Capitán, M., Fernández-Sánchez, C., Gomes, M. T. S. R., Rudnitskaya, A., and Jimenez-Jorquera, C., Thin-film electrochemical sensor for diphenylamine detection using molecularly imprinted polymers. *Anal. Chim. Acta* **809**, 141–147, DOI: https://doi.org/10.1016/j.aca.2013.11.038 (2014).
24. Alizadeh, N. and Farokhcheh, A. Simultaneous determination of diphenylamine and nitrosodiphenylamine by photochemically induced fluorescence and synchronous fluorimetry using double scans method. *Talanta* **121**, 239–246, DOI: https://doi.org/10.1016/j.talanta.2013.11.054 (2014).
25. Drzyzga, O. Diphenylamine and derivatives in the environment: a review. *Chemosphere* **53**, 809–818, DOI: https://doi.org/10.1016/S0045-6535(03)00613-1 (2003).
26. Rezaei, F., Yamini, Y., Asiabi, H., and Moradi, M. Determination of diphenylamine residue in fruit samples by supercritical fluid extraction followed by vesicular based-supramolecular solvent microextraction. *J. Supercrit. Fluids* **100**, 79–85, DOI: https://doi.org/10.1016/j.supflu.2015.02.021 (2015).
27. Sholberg, P. L., Harlton, C., Haag, P., Lévesque, C. A., O'Gorman, D., and Seifert, K., Benzimidazole and diphenylamine sensitivity and identity of Penicillium spp. that cause postharvest blue mold of apples using β-tubulin gene sequences. *Postharvest Biol. Technol.* **36**, 41–49, DOI: https://doi.org/10.1016/j.postharvbio.2004.07.011 (2005).

28. Drouillet-Pinard, P., Boisset, M., Periquet, A., Lecerf, J. M., Casse, F., Catteau, M., Barnat, S. Realistic approach of pesticide residues and French consumer exposure within fruit & vegetable intake. *J. Environ. Sci. Heal. B* **46**, 84–91, DOI: https://doi.org/10.1080/03601234.2011.534413 (2010).
29. Jelisavac, L. and Filipovic, M. Determination of diphenylamine and its mono-derivatives in single-base gun propellants during aging by high performance liquid chromatography. *Chromatographia* **55**, 239–241, DOI: https://doi.org/10.1007/BF02492149 (2002).
30. Curtis, N. J. and Rogasch P. E. Determination of Derivatives of Diphenylamine in Australian Gun Propellants by high performance liquid chromatography. *Propellants, Explos. Pyrotech.* **12**, 158–163, DOI: https://doi.org/10.1002/prep.19870120505 (1987).
31. Song, J., Forney, C. F., and Jordan, M. A. A method to detect diphenylamine contamination of apple fruit and storages using headspace solid phase micro-extraction and gas chromatography/mass spectroscopy. *Food Chem.*, **160**, 255–259, DOI: https://doi.org/10.1016/j.foodchem.2014.03.099 (2014).
32. Ahmad, A., Qureshi, M., Khan, I. A., and Alam, K. Z. Spectrophotometric Determination of Diphenylamine, Pyrrole, and Indole - A Kinetic Study. *Anal. Lett.* **23**, 1139–1157, DOI: https://doi.org/10.1080/00032719008053452 (1990).
33. Adawyia, J. H., Alwan, M. A., and Allaa, A. J. Optimizing of porous silicon morphology for synthesis of silver nanoparticles. *Micropor. Mesopor. Mat.*, **227**, 152–160, DOI: https://doi.org/10.1016/j.micromeso.2016.02.035 (2016).
34. Harraz, F. A., Tsuboi, T., Sasano, J., Sakka, T., and Ogata, Y. H. Metal Deposition onto a Porous Silicon Layer by Immersion Plating from Aqueous and Nonaqueous Solutions. *J. Electrochem. Soc.* **149**, C456, DOI: https://doi.org/10.1149/1.1498841 (2002).
35. Len'shin, A. S., Kashkarov, V. M., Turishchev, S. Y., Smirnov, M. S., and Domashevskaya, E. P. Effect of natural aging on photoluminescence of porous silicon. *Tech. Phys. Lett.* **37**, 789–792, DOI: https://doi.org/10.1134/S1063785011090124 (2011).
36. Sinha, S., Piekiel, N. W., Smith, G. L., and Morris, C. J. Investigating aging effects for porous silicon energetic materials. *Combust. Flame* **181**, 164–171, DOI: https://doi.org/10.1016/j.combustflame.2017.03.015 (2017).
37. Zeiri, L., Rechav, K., Porat, Z., and Zeiri, Y. Silver Nanoparticles Deposited on Porous Silicon as a Surface-Enhanced Raman Scattering (SERS) Active Substrate. *Appl. Spectrosc.* **66**, 294–299, DOI: https://doi.org/10.1366/11-06476 (2012).
38. Chattopadhyay, S., Jana, P., Mitra, A., Sarkar, S. K., Ganguly, T., and Mallick, P. K. Raman excitation profiles and molecular structures in the excited electronic states of 2,2'-dipyridylamine. *J. Raman Spectrosc.* **28**, 559–565, DOI: https://doi.org/10.1002/(SICI)1097-4555(199708)28:8<559::AID-JRS113>3.0.CO;2-R (1997).
39. Sett, P., Chattopadhyay, S., and Mallick, P. K. Excited state molecular configuration of biphenyl. *Chem. Phys. Lett.* **331**, 215–223, DOI: https://doi.org/10.1016/S0009-2614(00)01173-8 (2000).

40. Sett, P., Chattopadhyay, S., and Mallick, P. K. Raman Excitation Profiles and Excited State Molecular Configurations of Three Isomeric Acetylpyridines and Acetophenone. *J. Mol. Spectrosc.* **202**, 24–36, DOI: https://doi.org/10.1006/jmsp.2000.8081 (2000).
41. Thayer, E., Turner, W., Blama, S., Devada, M. S. s, and Hondrogiannis, E. M. Signal detection limit of a portable Raman spectrometer for the SERS detection of gunshot residue. *MRS Commun.* **9**, 948–955, DOI: https://doi.org/10.1557/mrc.2019.100 (2019).
42. Hande, P. E., Samui, A. B., and Kulkarni, P. S. An Efficient Method for Determination of the Diphenylamine (Stabilizer) in Propellants by Molecularly Imprinted Polymer based Carbon Paste Electrochemical Sensor. *Propellants, Explos. Pyrotech.* **42**, 376–380, DOI: https://doi.org/10.1002/prep.201600118 (2017).
43. Liu, L., Zhu, X., Zeng, Y., Wang, H., Lu, Y., Zhang, J., Yin, Z., Chen, Z., Yang, Y., Li, L., An Electrochemical Sensor for Diphenylamine Detection Based on Reduced Graphene Oxide/Fe3O4-Molecularly Imprinted Polymer with 1,4-Butanediyl-3,3'-bis-l-vinylimidazolium Dihexafluorophosphate Ionic Liquid as Cross-Linker. *Polymers (Basel).* **10**, 1329, DOI: https://doi.org/10.3390/polym10121329 (2018).
44. Commission Regulation (EU) 2016/67, https://www.legislation.gov.uk/eur/2016/67/data.xht?view=snippet&wrap=true

Figures

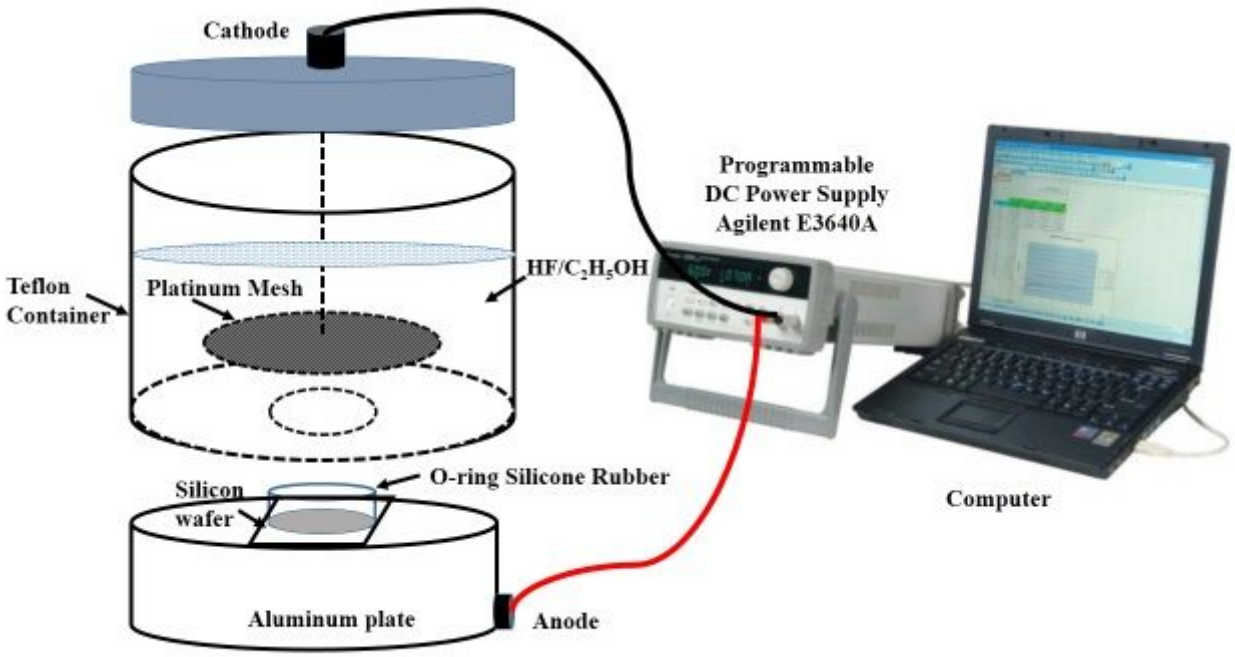

Figure 1

Experimental set up of etching process for formation of PSi.

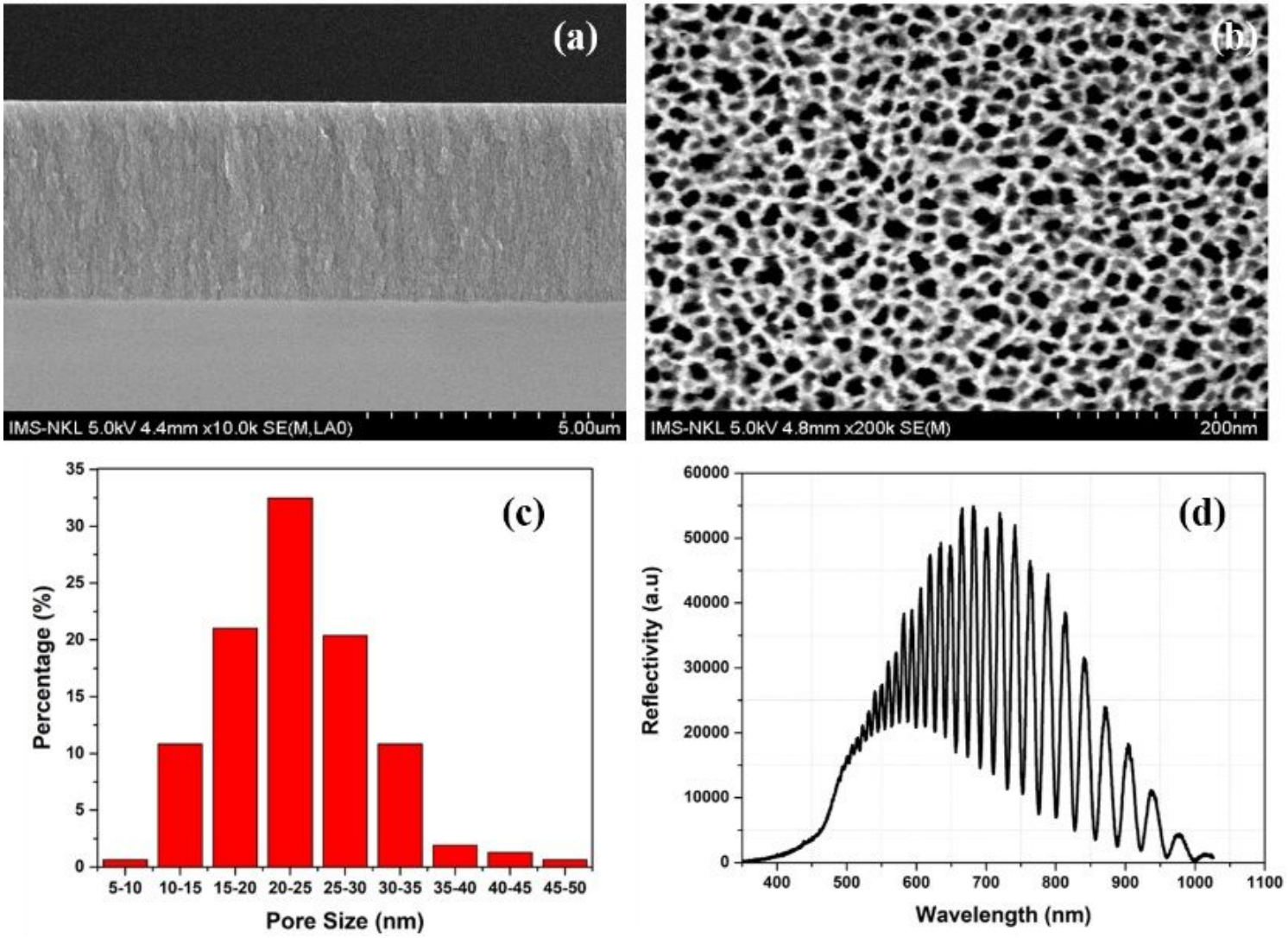

Figure 2

SEM images of the PSi structure obtained from etching process for 2 minutes at current density of 50 mA/cm2: (a) cross-section, (b) surface morphology, (c) pore size distributions, and (d) Reflectance spectrum of PSi.

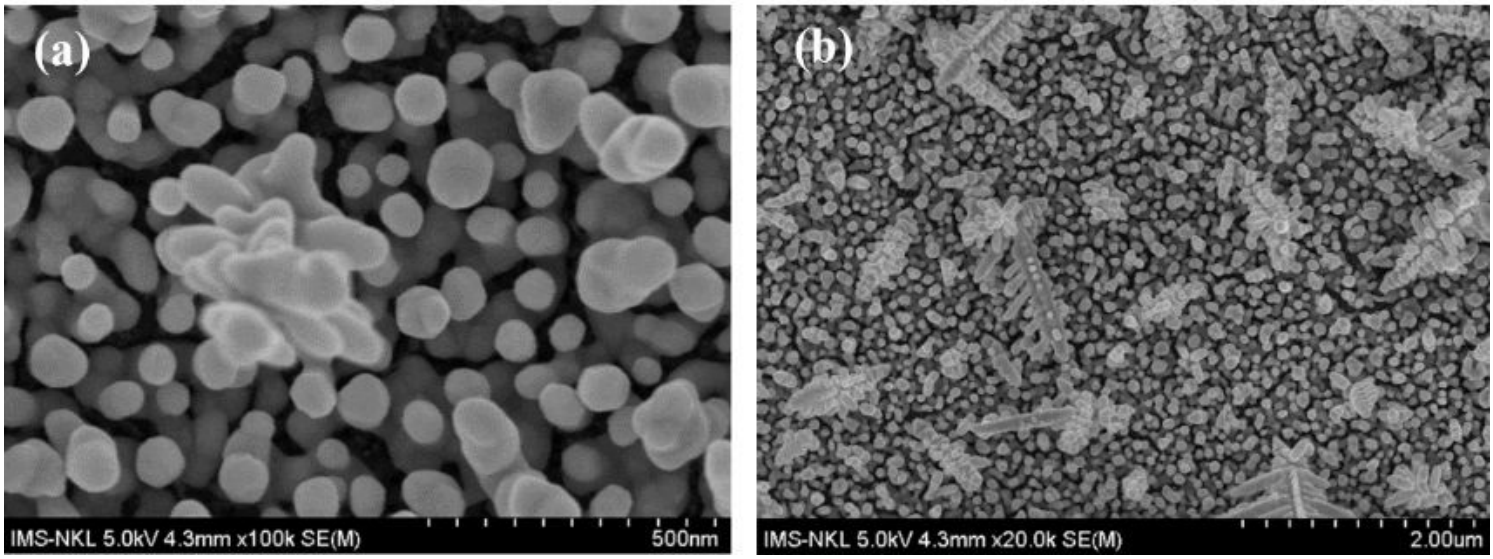

Figure 3

Morphology of AgNPs deposited on the silicon surface after 2 minutes immersed into 4.8 M HF and 10-2 M AgNO3 solution. The flower-like (a) and dendrite (b) morphologies of nano-silver were obtained on the silicon surface.

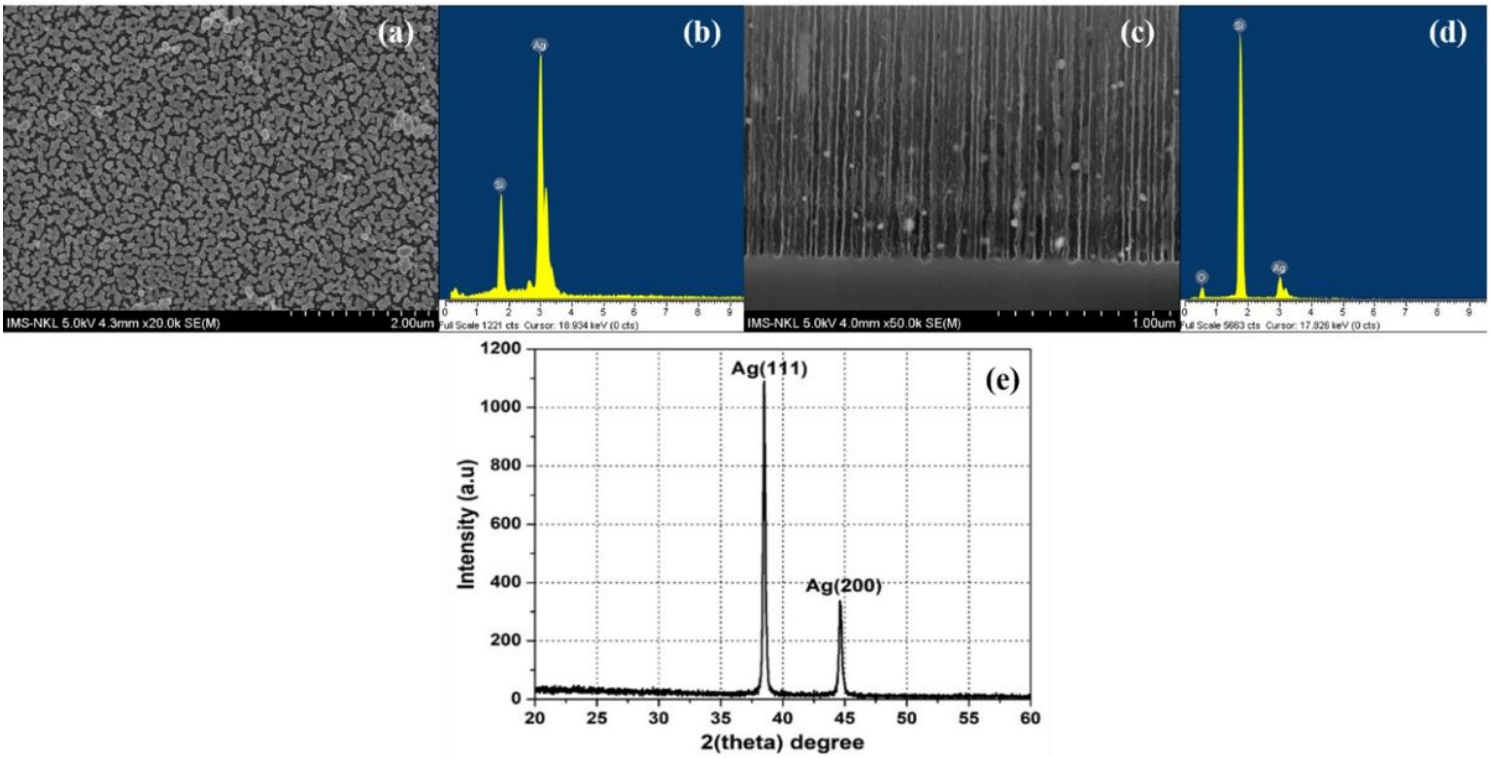

Figure 4

SEM images and EDX analysis of AgNPs on PSi surface (a,b), and of AgNPs on PSi-nanopillars (c,d) for the hybrid Ag/PSi samples prepared by immersion plating of bare PSi samples into 1mM AgNO3 solution for 20 min at room temperature (e) XRD analysis of AgNPs on the PSi surface.

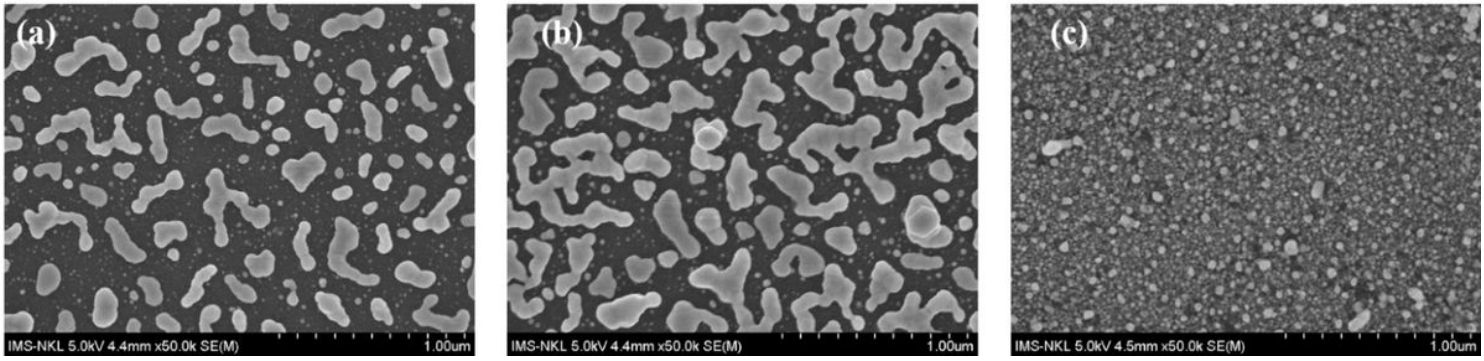

Figure 5

Effect of the deposition duration on morphology of the silver-decorated PSi: (a) 5 min, (b) 10 min and (c) 30 min.

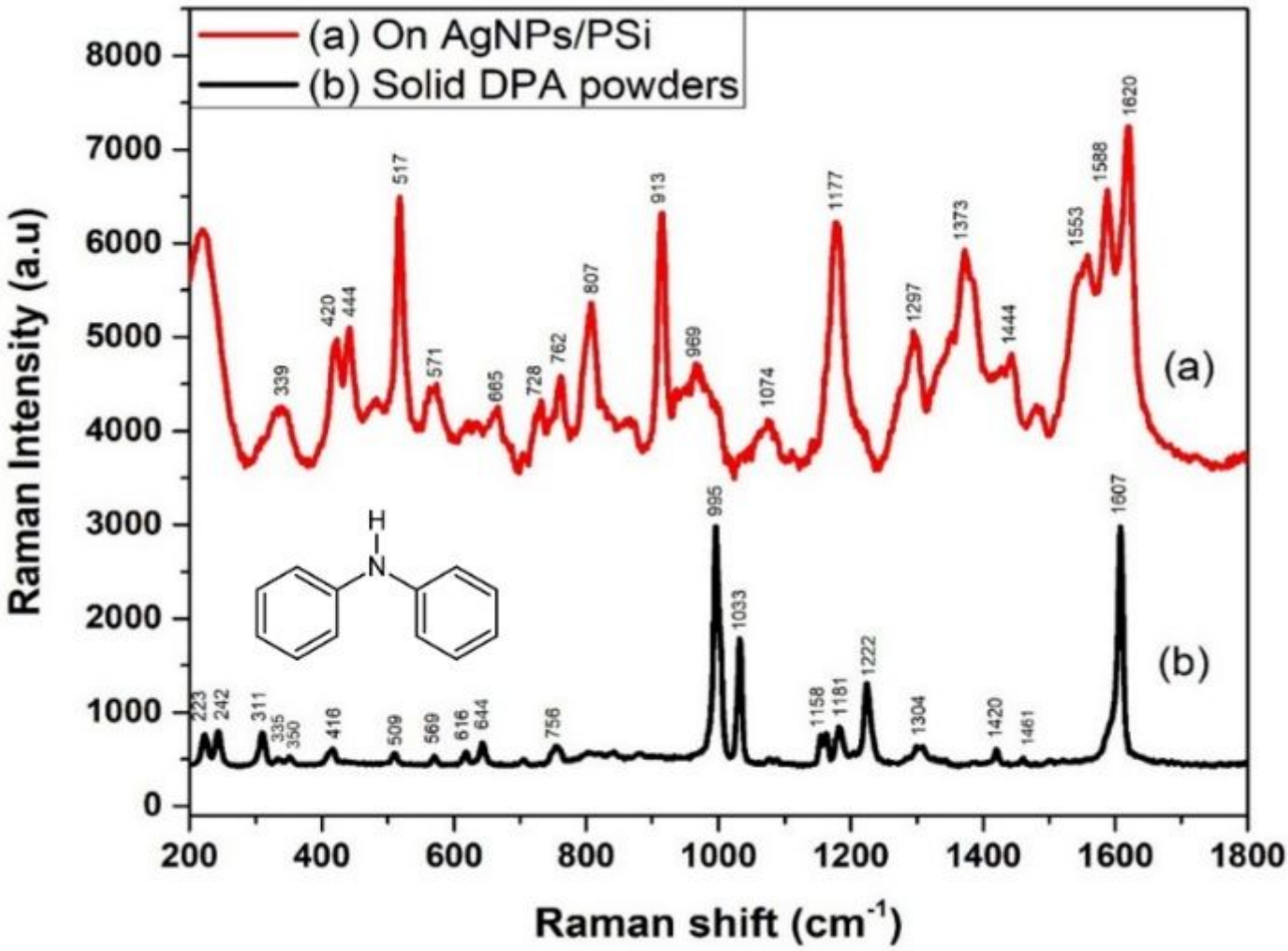

Figure 6

Raman spectra from DPA: (a) Raman spectrum of DPA with concentration of 10-3M measured by AgNP/PSi SERS, and (b) Raman spectrum of solid DPA measured without SERS. Inset: Molecular structure of DPA.

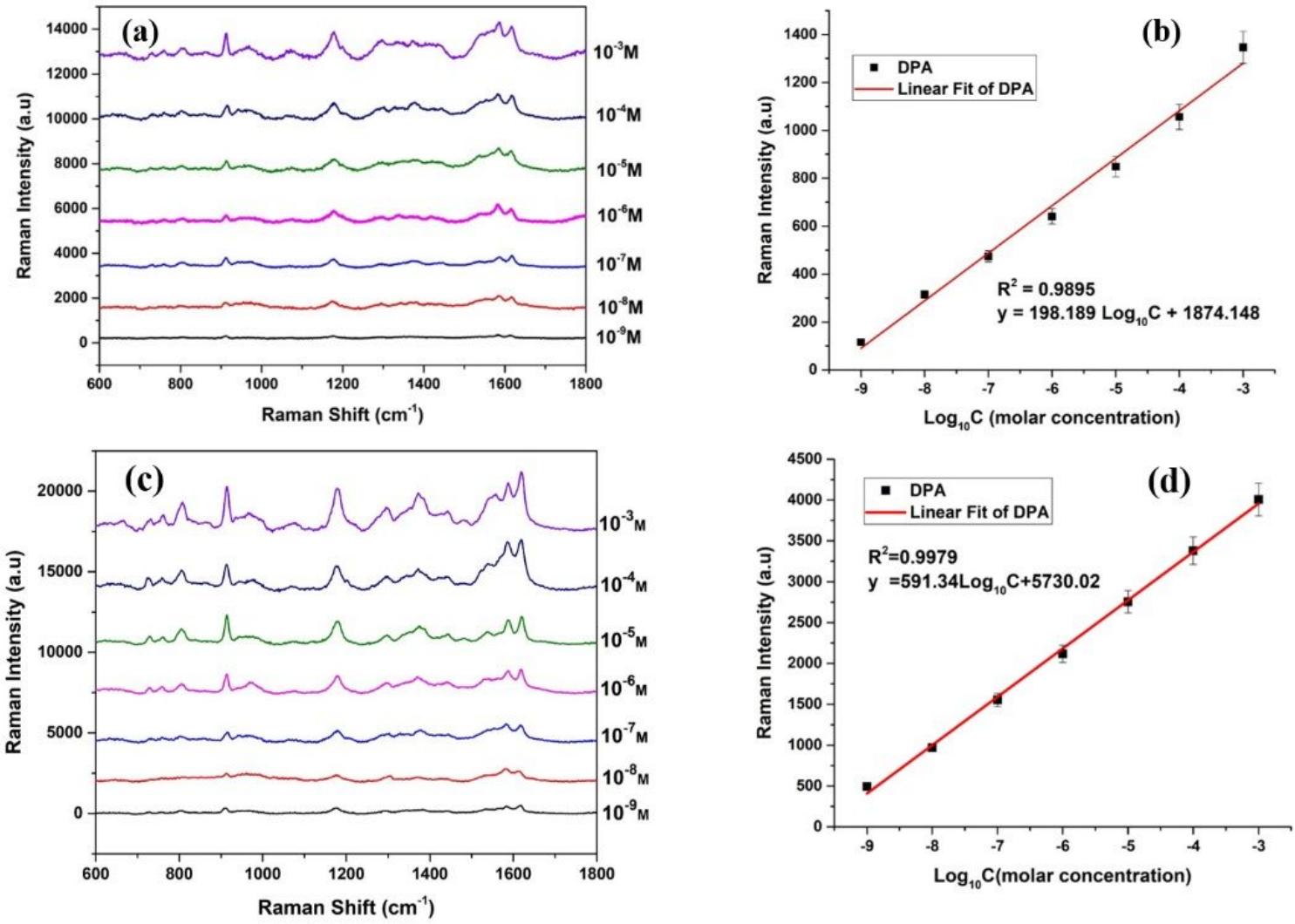

Figure 7

SERS spectra of DPA with the concentration of 10-9-10-3 M on the AgNPs/Si (a) and on AgNPs/PSi substrates (c). Linear fitting of Raman intensity at 1620 cm-1 with logarithm of DPA concentrations absorbed on AgNPs/Si (b) and on AgNPs/PSi (d).

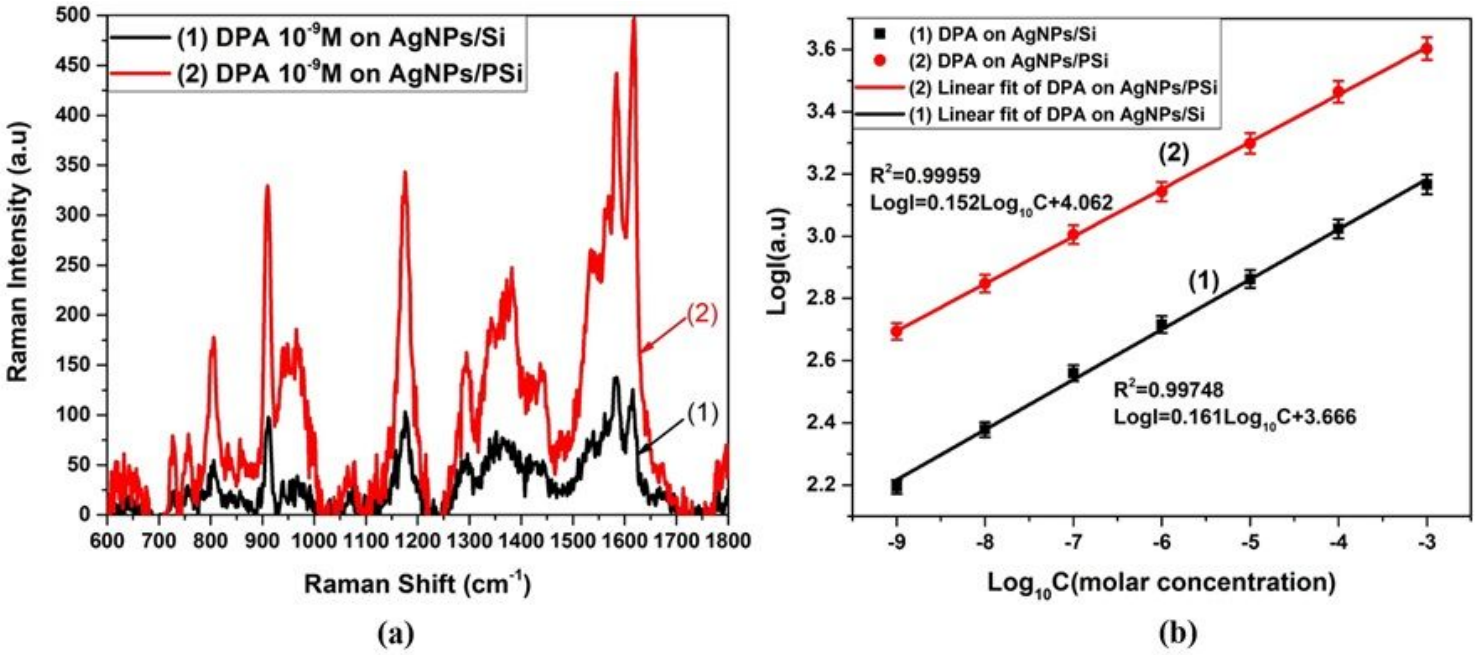

Figure 8

(a) SERS spectra of DPA with a concentration of 10-9 M adsorbed on the AgNPs/Si (line 1) and AgNPs/PSi (line 2). (b) Dependence in logarithmic scale of Raman intensity at 1620 cm-1 upon DPA concentration in the range of 10-3-10-9 M adsorbed on AgNPs/Si and on AgNPs/PSi.